Incremental Low-Rank Dynamic Mode Decomposition Model for Efficient Forecast Dissemination and Onboard Forecasting

T. Ryu[a], W. H. Ali[a], P. J. Haley, Jr.[a], C. Mirabito.[a], A. Charous[a], P. F. J. Lermusiaux[a,†]
[a] *Department of Mechanical Engineering, Massachusetts Institute of Technology, Cambridge, MA*
[†]Corresponding Author: pierrel@mit.edu

OCEANS 2022, Hampton Roads | 978-1-6654-6809-1/22/$31.00 ©2022 IEEE | DOI: 10.1109/OCEANS47191.2022.9977224

***Abstract*—Onboard forecasting is challenging but essential for unmanned autonomous ocean platforms. Due to the numerous operational constraints of these platforms, efficient adaptive Reduced-Order Models (ROMs) are needed. In this work, we employ the incremental Low-Rank Dynamic Mode Decomposition (iLRDMD), which is an adaptive, data-driven, DMD-based ROM that enables efficient forecast compression, transmission, and onboard forecasting. We demonstrate the algorithm on 3D multivariate Hybrid Coordinate Ocean Model (HYCOM) ocean fields in the Middle Atlantic Ridge (MAR) region. We further demonstrate that these iLRDMD ocean forecasts can be used for interdisciplinary applications such as underwater acoustics predictions. Here, acoustics fields computed from the ocean iLRDMD forecasts are compared to those computed from HYCOM fields. We also illustrate the application of a joint ocean-acoustics iLRDMD model for predetermined acoustics configurations. In the MAR region, we find that iLRDMD models are sufficiently accurate and efficient for onboard ocean and acoustic forecasting of temperature, salinity, velocity, and transmission loss fields.**

***Index Terms*—reduced-order model, Dynamic Mode Decomposition, forecast dissemination, communication, AUVs, autonomy, underwater acoustics**

I. Introduction

For many unmanned autonomous platforms at sea, sufficiently accurate forecasts of the ocean states are crucial for parts of its missions such as ocean monitoring, path planning, or underwater acoustics computations [1]–[3]. Due to the operational constraints such as onboard power, memory, communication bandwidth, and space limitations, autonomous platforms cannot run high-fidelity numerical ocean simulations onboard. Therefore, a sufficiently accurate and efficient reduced-order model (ROM) is needed for reliable onboard forecasting of the ocean. In previous works such as [4], [5], the Dynamical Mode Decomposition (DMD) model [6]–[10] was demonstrated to be an accurate ocean ROM for a relatively short time period. However, as the DMD model is limited to linearly approximating the underlying dynamics, its forecast accuracy was shown to decay over time [4], [5], especially without updates from remote forecasting centers. To address several of these challenges specific to ocean applications, we employ the iLRDMD algorithm [3], [11]. The iLRDMD is an adaptive ROM that updates the onboard DMD model with new high-fidelity forecasts from numerical ocean simulations computed and transmitted from remote centers. Specifically, it uses the Proper Orthogonal Decomposition (POD) and DMD for efficient compression and transmission of the high-fidelity forecasts and the subsequent update of the onboard DMD model from the compressed forecasts. Finally, the onboard iLRDMD model can be used to provide onboard forecasts for the autonomous platforms.

In this work, we build upon our previous evaluation of the iLRDMD algorithm with an univariate 2D flow behind a cylinder test case [11] and demonstrate the iLRDMD algorithm on multivariate 3D ocean physics and acoustics applications. For the ocean physics, we utilize the Hybrid Coordinate Ocean Model (HYCOM) hindcast from January and February of 2020 in the North Atlantic domain ran by the Naval Research Laboratory [12]–[14]. This was a similar run to the Global Ocean Forecasting System 3.1 reanalysis that spanned 1994-2021 [15]. The HYCOM forecasts were 1/12.5 deg two-way coupled to the Los Alamos Community Ice Code and used the Navy Coupled Ocean Data Assimilation [16], [17] for data assimilation. The National Centers for Environmental Prediction Climate Forecast System Reanalysis - Version 2 [18], [19] was used for the atmospheric forcing. We train the iLRDMD model on a region around an ocean cross-section of interest near the Middle Atlantic Ridge (MAR). We explore the feasibility of using the iLRDMD ocean forecasts for underwater acoustics computations. The iLRDMD model's salinity and temperature forecasts are first used to compute the sound speed field. This is then used as an input for the acoustic Multidisciplinary Simulation, Estimation, and Assimilation Systems (MSEAS) - Parabolic Equation framework (MSEAS-ParEq) [20], [21] to compute the acoustic pressure and transmission loss (TL) fields. Finally, we explore the use and accuracy of a joint ocean-acoustics iLRDMD model. This has the potential of more efficiently reducing and forecasting joint ocean-acoustics fields for predetermined acoustics configurations.

II. Incremental Low-Rank DMD (iLRDMD)

The iLRDMD algorithm enables the efficient compression and transmission of high-fidelity numerical ocean simulations from remote centers and the subsequent update of the onboard DMD model for onboard forecasting [3], [11]. The iLRDMD algorithm accomplishes this by: i) projecting the full-dimensional, high-fidelity ocean forecasts computed at remote centers onto POD bases and transmitting them to the autonomous platforms; ii) updating the onboard DMD model using the compressed ocean forecasts in the reduced space; iii) providing ocean forecasts in the full-dimensional physical space; and iv) over longer times, as the underlying dynamics change significantly, updating the POD bases on the remote

centers and communicating it to the platforms. The novelty of the iLRDMD algorithm comes from how it efficiently uses the POD-compressed ocean forecasts to update the onboard DMD model without having to reconstruct the full-dimensional state. The full-dimensional states only need to be reconstructed when onboard forecasting is needed.

In the following sections, we summarize the components of the iLRDMD algorithm including the DMD, low-rank DMD, incremental DMD [22], and incremental POD algorithms [23], [24]. More detailed explanations of each of the components can be found in [3].

A. Dynamic Mode Decomposition (DMD)

In this section, we first briefly review the DMD algorithm developed in [6]–[10] as it serves as the underpinning for the iLRDMD algorithm. The following description of DMD closely follows that of [6] and is given in the same notation as in [3]. The DMD algorithm typically considers snapshot matrices

$$\mathbf{X} = \begin{bmatrix} \mathbf{x}_1 & \mathbf{x}_2 & \cdots & \mathbf{x}_{n_t-1} \end{bmatrix} \tag{1}$$

and

$$\mathbf{X}' = \begin{bmatrix} \mathbf{x}_2 & \mathbf{x}_3 & \cdots & \mathbf{x}_{n_t} \end{bmatrix}, \tag{2}$$

where $\mathbf{X}, \mathbf{X}' \in \mathbb{R}^{n_x \times (n_t-1)}$. For ocean applications, the individual state vectors of the snapshot matrices could, for example, be 2D univariate fields of sea surface temperature (SST) or 3D multivariate fields including u-velocity, v-velocity, salinity, temperature, and ocean free-surface stacked into a single (normalized) vector [25], [26].

The DMD algorithm then aims to find an operator $\mathbf{A}$ that is the solution to the following minimization problem

$$\min_{\mathbf{A}} ||\mathbf{X}' - \mathbf{A}\mathbf{X}||_F. \tag{3}$$

The optimal $\mathbf{A}$ can be shown to be

$$\mathbf{A} = \mathbf{X}^{'}\mathbf{X}^{\dagger}, \tag{4}$$

where $\mathbf{X}^{\dagger}$ is the Moore–Penrose pseudoinverse of $\mathbf{X}$ that can be computed using the n_r truncated singular value decomposition (SVD). With the following truncated SVD $\mathbf{X} \approx \mathbf{U}_{n_r}\mathbf{\Sigma}_{n_r}\mathbf{V}_{n_r}^T$, the matrices $\mathbf{U}_{n_r} \in \mathbb{R}^{n_x \times n_r}, \mathbf{\Sigma}_{n_r} \in \mathbb{R}^{n_r \times n_r}$, and $\mathbf{V}_{n_r} \in \mathbb{R}^{(n_t-1)\times n_r}$, where $n_r \ll n_x, n_t$, the pseudoinverse of $\mathbf{X}$ is $\mathbf{X}^{\dagger} \approx \mathbf{V}_{n_r}\mathbf{\Sigma}_{n_r}^{-1}\mathbf{U}_{n_r}^T$.

In practice [6], for computational efficiency, we often compute $\tilde{\mathbf{A}}$, that is the $n_r \times n_r$ projection of $\mathbf{A}$ onto the POD modes $\mathbf{U}_{n_r}$ and that can be written as

$$\tilde{\mathbf{A}} = \mathbf{U}_{n_r}^T\mathbf{A}\mathbf{U}_{n_r}. \tag{5}$$

B. Forecast Dissemination and Low-Rank DMD

The iLRDMD algorithm obtains efficient and accurate compression of the full-dimensional ocean forecasts by projecting them onto a set of POD bases. These compressed states $\mathbf{Z}, \mathbf{Z}' \in \mathbb{R}^{n_r \times (n_t-1)}$ are defined as

$$\mathbf{Z} = \mathbf{U}_{n_r}^T\mathbf{X}, \quad \mathbf{Z}' = \mathbf{U}_{n_r}^T\mathbf{X}'. \tag{6}$$

The DMD operator defined from the minimization problem

$$\min_{\mathbf{A}_z} ||\mathbf{Z}' - \mathbf{A}_z\mathbf{Z}||_F \tag{7}$$

can be shown as in [3] to be equivalent to $\tilde{\mathbf{A}}$ defined in eq. 5. Defining the low-rank DMD in such a way means that the DMD operator can be efficiently built from the compressed states $\mathbf{Z}, \mathbf{Z}'$. Then, once the onboard forecasts are needed, the pre-loaded or communicated POD bases are used to reconstruct the full-dimensional states.

C. Weighted Incremental DMD (iDMD)

The iLRDMD algorithm starts from the low-rank DMD and aims to update the onboard DMD model with new compressed states. The novelty of the iLRDMD algorithm lies in that the iDMD [22] update is done in the compressed state space and not in the full-dimensional state space. Consider the DMD operator $\mathbf{A}_{z,n_t-1}$ that is defined for the compressed states

$$\mathbf{Z}_{n_t-1} = \begin{bmatrix} \rho^{n_t-2}\mathbf{z}_1 & \rho^{n_t-1}\mathbf{z}_2 & \cdots & \mathbf{z}_{n_t-1} \end{bmatrix}, \tag{8}$$

$$\mathbf{Z}_{n_t-1}^{'} = \begin{bmatrix} \rho^{n_t-2}\mathbf{z}_2 & \rho^{n_t-1}\mathbf{z}_3 & \cdots & \mathbf{z}_{n_t} \end{bmatrix}, \tag{9}$$

where $\rho \in [0, 1]$ is the forgetting rate [22], [27], [28]. Given a set of new state vectors $(\mathbf{z}_{n_t}, \mathbf{z}_{n_t+1})$, the iDMD algorithm [22] gives a set of efficient update equations to obtain the DMD operator $\mathbf{A}_{z,n_t}$ that is defined for

$$\mathbf{Z}_{n_t} = \begin{bmatrix} \rho^{n_t-1}\mathbf{z}_1 & \rho^{n_t}\mathbf{z}_2 & \cdots & \rho\mathbf{z}_{n_t-1} & \mathbf{z}_{n_t} \end{bmatrix}, \tag{10}$$

$$\mathbf{Z}_{n_t}^{'} = \begin{bmatrix} \rho^{n_t-1}\mathbf{z}_2 & \rho^{n_t}\mathbf{z}_3 & \cdots & \rho\mathbf{z}_{n_t} & \mathbf{z}_{n_t+1} \end{bmatrix}. \tag{11}$$

D. Incremental POD (iPOD)

As the underlying dynamics change significantly, the compression accuracy of new forecasts onto the set of pre-trained POD bases decays. This could be alleviated by having a more robust set of POD bases to begin with. However, the iLRDMD algorithm utilizes the high-fidelity forecasts on remote centers to update the POD bases. Fundamentally, the iPOD algorithm [23], [24] aims to start from the SVD of

$$\mathbf{X}_k \approx \mathbf{U}_{x_k}\mathbf{\Sigma}_{x_k}\mathbf{V}_{x_k}^T, \tag{12}$$

with $\mathbf{X_k} \in \mathbb{R}^{n_x \times k}$ and obtain the components of the SVD of $\mathbf{X}_{k+1}$:

$$\mathbf{X}_{k+1} \approx \mathbf{U}_{x_{k+1}}\mathbf{\Sigma}_{x_{k+1}}\mathbf{V}_{x_{k+1}}^T, \tag{13}$$

with simple update equations to the individual components $\mathbf{U}_{x_k}, \mathbf{\Sigma}_{x_k}$, and $\mathbf{V}_{x_k}$.

III. Underwater Acoustics Computations

Underwater acoustics computation and prediction is fundamentally complex due to the myriad of processes such as internal tides, waves, fronts, eddies, surface dynamics, and air-to-sea interactions that affect sound propagation on a wide range of temporal and physical scales [29]–[36]. Previous results in our group [20], [21], [33], [36]–[44] have employed ensemble and dynamically-orthogonal equations to predict ocean physical-acoustical field probabilities and complete multivariate joint Bayesian estimation and inversion of physical-acoustical fields.

To predict underwater acoustics performance from hours to days or weeks into the future, one can utilize regional and global ocean forecasts computed from numerical data-assimilating ocean modeling systems. In this work, to allow acoustic forecasting onboard ocean vehicles, we explore the use of the iLRDMD ocean forecasts for deterministic underwater acoustics forecasting. As previously outlined, the 3D multivariate ocean iLRDMD forecasts of the temperature and salinity fields are first used to compute the sound speed fields. These are subsequently used as inputs for the acoustic MSEAS-ParEq model [20], [21]. Another method to predict underwater acoustics performance into the future is to augment the ocean state vectors with acoustics variables for a joint ocean-acoustics iLRDMD. This would be particularly useful when the platform has a predefined use case with a set source type and location, receiver location, ocean section, etc.

IV. Applications

In this work, we demonstrate the iLRDMD algorithm on the HYCOM hindcast fields in the North Atlantic domain [12], [13]. The HYCOM hindcast fields on January and February 2020 are given every 3 hours. Here, since the goal is to reduce the HYCOM hindcast fields, they are considered as the ground truth against which we compare our reduced-order iLRDMD forecasts. Similarly, for underwater acoustics computations results, the acoustics field computed from the ocean iLRDMD forecasts are compared to those computed from HYCOM fields.

A. 3D multivariate Ocean iLRDMD forecasts

For building the 3D multivariate iLRDMD model, we consider the u-velocity, v-velocity, temperature, and salinity fields in a smaller region of interest marked by the black box in figure 1. This encompasses the 240 km ocean section with the source and frequency location marked by the red line in figure 1. Defining this physical subdomain of influence around the ocean section enables the iLRDMD model to capture the scales of dynamics that are relevant for the ocean acoustics section. Note that the goal of the 3D multivariate iLRDMD model is to provide onboard forecasting of salinity and temperature to be used for the subsequent underwater acoustics computations.

We employ the first 380 three-hourly HYCOM fields for training with a forgetting rate of 0.7. The POD-compressed forecast states are assumed to be received every 24 hours in the form of forecast coefficients. The more expensive transmission of the updated POD bases is assumed to occur every 96 hours. Finally, we only use 379 POD modes for compression and transmission, resulting in a compressed file size of 3.03 kB. In comparison, the original smaller subdomain has corresponding grid point sizes of $101 \times 89 \times 101$ (lat, lon, depth), resulting in a full-dimensional file size of 7.26 MB. This is approximately equivalent to a 2395:1 compression ratio.

We now demonstrate the accuracy of the 3D multivariate iLRDMD ocean forecasts of temperature and salinity in figures 2 and 3 respectively, using the Pattern Correlation Coefficients

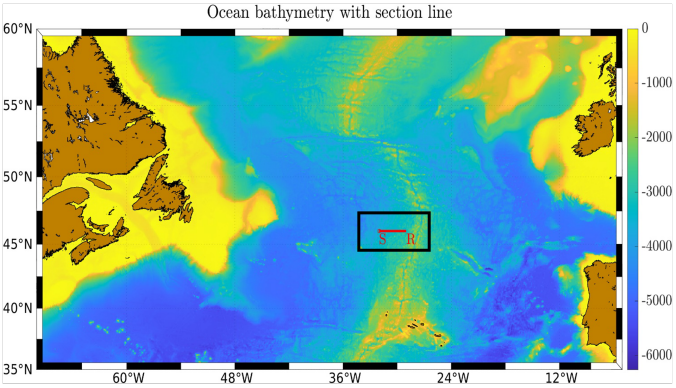

Fig. 1. HYCOM's ocean bathymetry in the North Atlantic region with a 240 km ocean section near the Middle Atlantic Ridge (MAR) domain (red line) and the relevant ocean region of influence (black box). he source and receiver locations are marked by 'S' and 'R', respectively.

(PCC). The PCC is a time mean subtracted pattern coefficient [45] where 1 means perfect correlation, 0 means no correlation, and -1 means anti-correlation, between a target signal and its predicted estimate. It can be seen from both of the figures that the PCC initially slowly decays over time until about 0.6 to 0.7 until it sharply recovers when the POD bases is updated. The decay in PCC is indeed due to the POD bases no longer being as accurate in the compression and transmission of new forecasts. Although the iLRDMD model is being updated with compressed forecasts, as the compression bases becomes more inaccurate, the iLRDMD forecasts' accuracy continues to decay. Once the updated POD bases are communicated and the new forecasts are compressed accurately once again, the iLRDMD forecasts recover a higher level of accuracy. This corresponds to the sharp recovery of the PCC values.

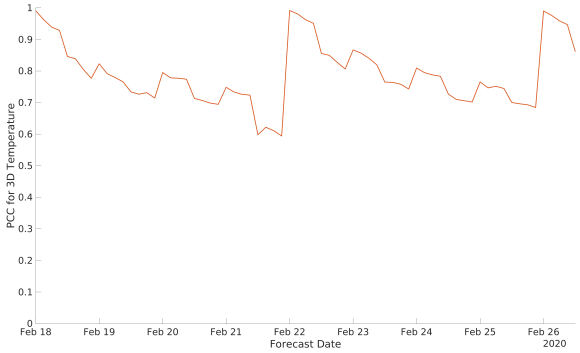

Fig. 2. PCC evolution over time of the 3D multivariate iLRDMD forecasts of temperature

The PCC values correspond to the error fields in the physical domain well. Figures 4, 5, and 6 show the error field of the SST in the region of interest on 2020 Feb. 18 03:00, Feb. 18 18:00, and Feb. 22 00:00 respectively. It can be seen that the errors initially increase over time from Feb. 18 03:00 to 18:00. This corresponds to the decrease in the PCC shown in figure 2. The SST field on Feb. 22 00:00 in figure 6 corresponds to the time at which the updated POD bases is communicated and

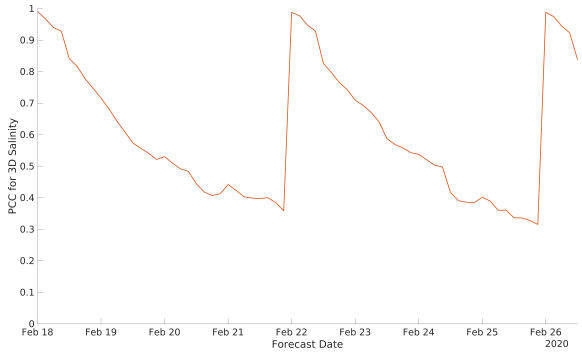

Fig. 3. PCC evolution over time of the 3D multivariate iLRDMD forecasts of salinity

the PCC recovers significantly in figure 2. It is clear that the PCC values are reflected in the overall error in the physical fields. Although only the error fields for SST were shown here, a similar trend can be observed for other ocean forecast variables and at different depths as well.

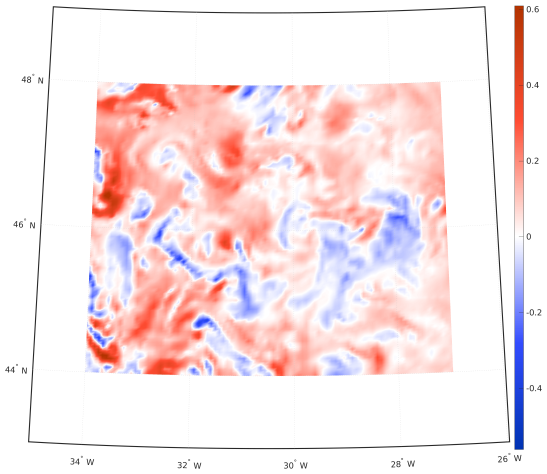

Fig. 4. Error field of SST in the region of interest on 2020 Feb. 18 03:00

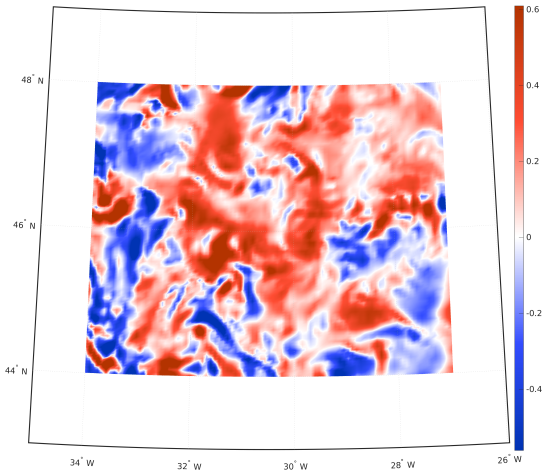

Fig. 5. Error field of SST in the region of interest on 2020 Feb. 18 18:00

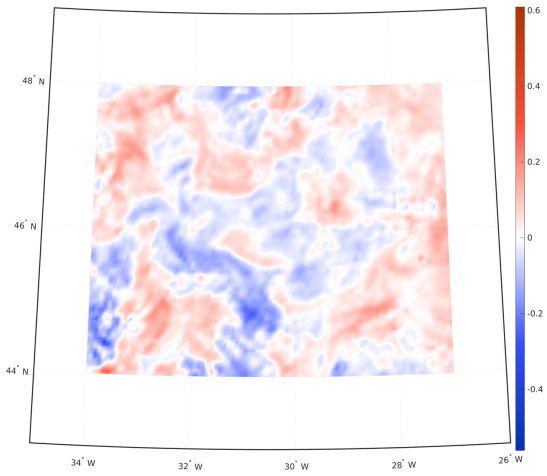

Fig. 6. Error field of SST in the region of interest on 2020 Feb. 22 00:00

B. iLRDMD ocean forecasts for underwater acoustics

Sound speed fields can be computed using the above reduced-order 3D multivariate iLRDMD forecasts of temperature and salinity. Figures 7, 8, and 9 show the temperature and the derived sound speed error fields ("heat maps") in the 240 km transect, at their respective times. As before, it can be seen that the errors initially increase over time from Feb. 18 03:00 to 18:00 in figures 7 and 8. However, once the updated POD bases allow the iLRDMD model to be updated with more accurately compressed forecasts, the error decreases in figure 9. It can also be seen that the errors are higher near the surface for the temperature error fields. This is in part because the 3D multivariate ocean iLRDMD model does not include variables that significantly affect the surface such as atmospheric forcing. A similar pattern of the error field is observed for sound speed since it is a derived quantity of temperature and salinity.

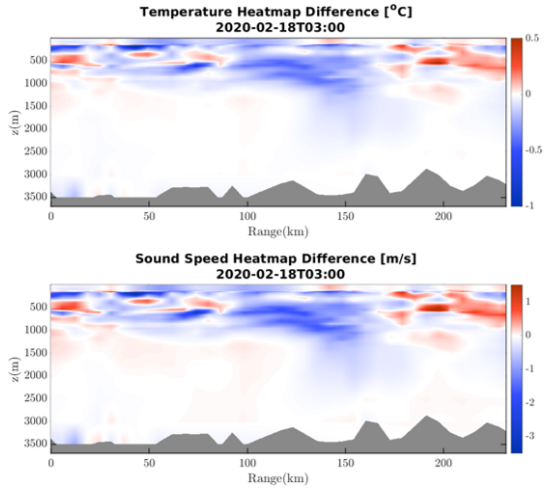

Fig. 7. Temperature and sound speed error fields ("heat maps") in the 240 km transect on 2020 Feb. 18 03:00

The sound speed fields obtained in the previous step can now finally be used as inputs for our MSEAS-ParEq model

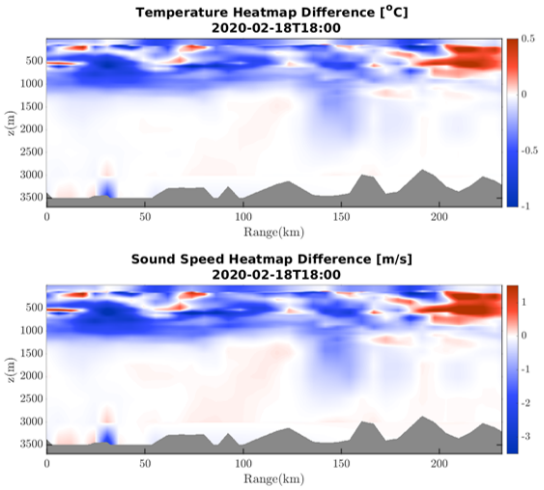

Fig. 8. Temperature and sound speed error fields ("heat maps") in the 240 km transect on 2020 Feb. 18 18:00

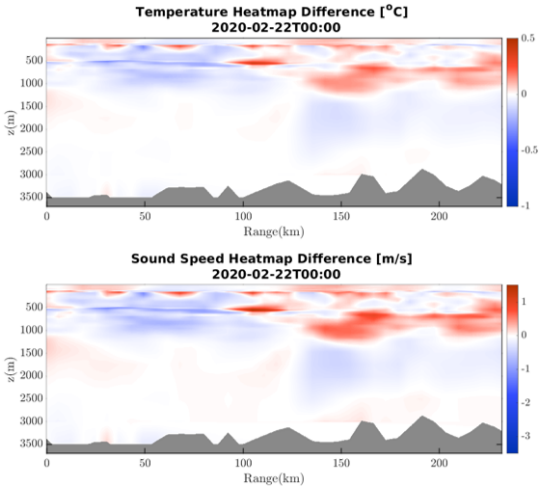

Fig. 9. Temperature and sound speed error fields ("heat maps") in the 240 km transect on 2020 Feb. 22 00:00

to compute acoustic pressure and TL fields. For the acoustics results, we assumed that we have an omni-directional source at 10 m depth on the left, which is marked by a pink dot in figure 10. We also assumed a receiver position at 50 m depth.

Figure 10 shows the TL fields computed based on HYCOM and iLRDMD ocean fields on 2020 Feb. 18 03:00. Qualitatively, we find that the TL fields computed from the reduced-order iLRDMD forecasts at both times look similar to those computed directly from the high-dimensional HYCOM fields. The sound channel locations also seem to be predicted at relatively correct locations. Fields at other times provide similar results (not shown).

We now take a further look into the errors between the TL fields computed from iLRDMD and HYCOM fields, as shown in Figures 11, 12, and 13. The TL errors on 2020 Feb. 18 03:00 in figure 11 seem to be concentrated near the surface or further down in range. However, on 2020 Feb. 18 18:00, more errors emerge both deeper in the ocean section and closer to the source. Finally, once the updated POD bases

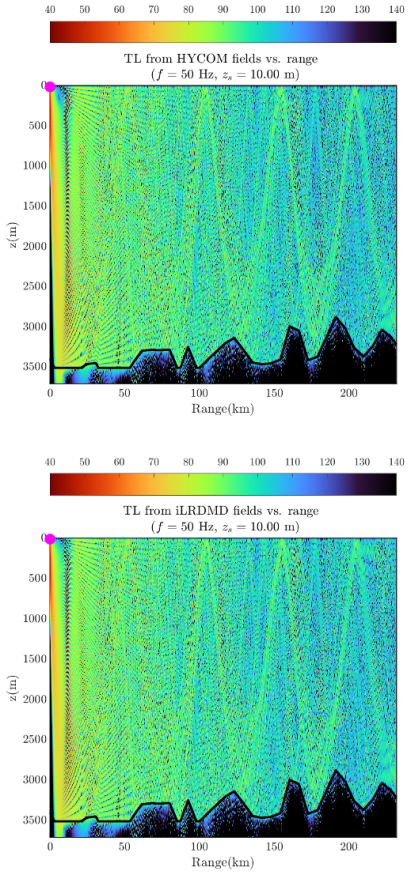

Fig. 10. Transmission loss (TL) fields computed from HYCOM and from reduced-order iLRDMD ocean fields in the 240 km transect on 2020 Feb. 18 03:00

are communicated and the iLRDMD ocean forecast recovers a high PCC, the TL errors also decrease significantly throughout the ocean section. Of course, in some underwater acoustic applications, there are error metrics more appropriate than the PCC or the root-mean-square-error of the continuous wave transmission loss. Here, we use PCC and error fields as an initial evaluation.

C. Joint ocean physics-acoustics iLRDMD forecasts

Finally, we demonstrate how a joint ocean-acoustics iLRDMD model could be utilized for onboard underwater acoustics forecasts. This could be particularly useful when the platform has a predefined use case that is of primary concern (e.g., a known set source type and location, receiver location, ocean section, etc.). The joint ocean-acoustics iLRDMD model is trained by augmenting the state vectors with TL fields computed based on HYCOM hindcasts within the same ocean acoustics section as in the previous examples. This joint forecast results in an increase in full-dimensional file sizes to around 33.86 MB. Upon projection onto the POD bases, the resulting compressed file size is 3.03 kB. This is approximately equivalent to a 11175:1 compression ratio.

The TL error fields from the joint ocean-acoustics iLRDMD forecasts on 2020 Feb. 18 03:00, 18:00, and Feb. 22 00:00 are

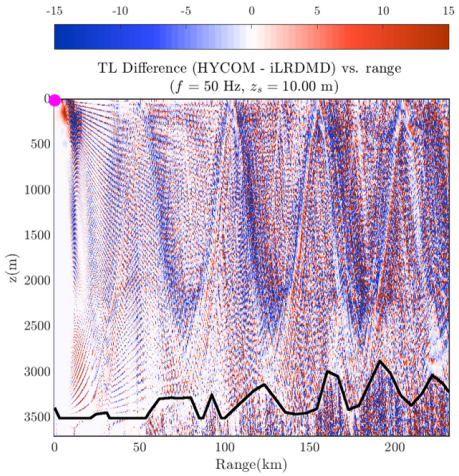

Fig. 11. Error field in TL computed from iLRDMD ocean forecasts in the 240 km transect on 2020 Feb. 18 03:00

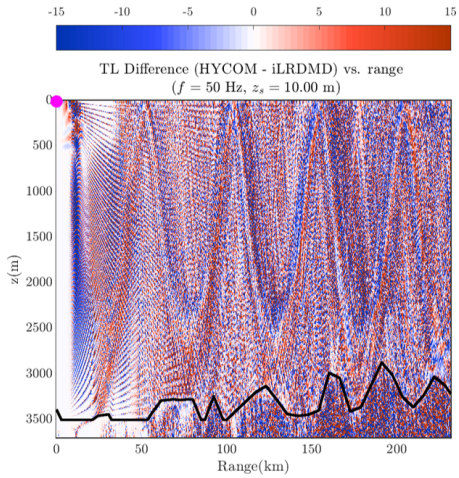

Fig. 12. Error field in TL computed from iLRDMD ocean forecasts in the 240 km transect on 2020 Feb. 18 18:00

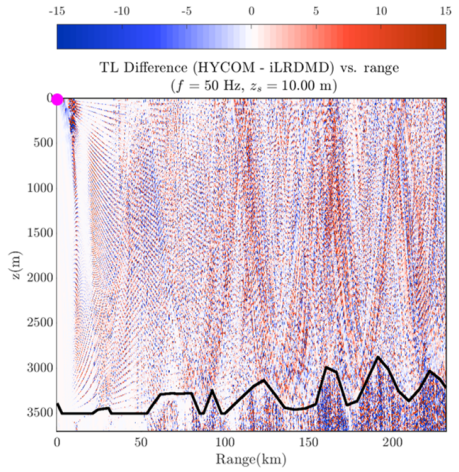

Fig. 13. Error field in TL computed from iLRDMD ocean forecasts in the 240 km transect on 2020 Feb. 22 00:00

shown in figures 14, 15, and 16. Most notably, while the TL errors based on ocean iLRDMD forecasts were concentrated near the surface, the TL errors based on the joint ocean-acoustics iLRDMD forecasts are relatively evenly distributed around the ocean section. Similarly to previous examples, the joint ocean-acoustics iLRDMD forecasts also show errors initially increasing until the POD bases are updated. Once the POD bases are updated, the errors decrease significantly, as shown in figure 16.

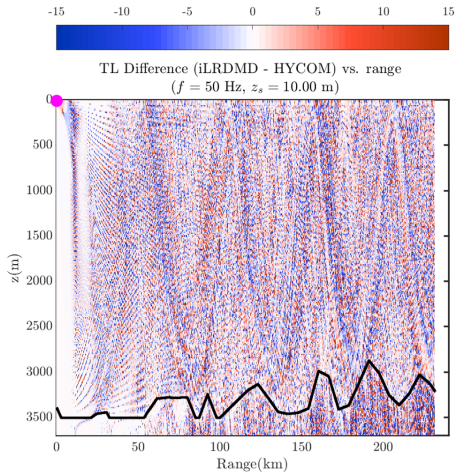

Fig. 14. Error field in TL computed from joint ocean-acoustics iLRDMD forecasts in the 240 km transect on 2020 Feb. 18 03:00

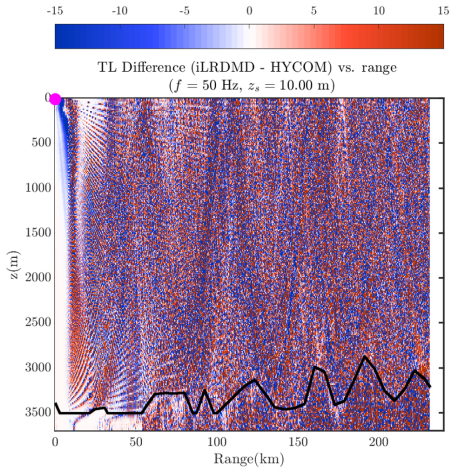

Fig. 15. Error field in TL computed from joint ocean-acoustics iLRDMD forecasts in the 240 km transect on 2020 Feb. 18 18:00

V. Conclusion and Future Work

In this work, we employed the iLRDMD algorithm, which allows the efficient compression and transmission of high-fidelity ocean forecasts, efficient updating of the DMD model using the compressed forecast coefficients, and, finally, on-board ocean forecasting. The application area was in the Middle Atlantic Ridge (MAR) region, using the global Hybrid Coordinate Ocean Model (HYCOM) reanalysis. The iLRDMD algorithm was utilized for simulated onboard forecasts of 3D multivariate ocean fields in this MAR domain. The iLRDMD

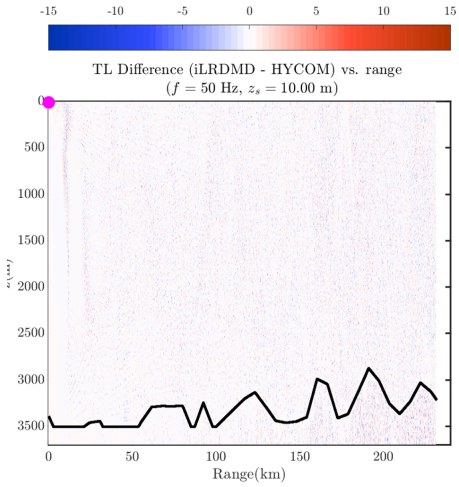

Fig. 16. Error field in TL computed from joint ocean-acoustics iLRDMD forecasts in the 240 km transect on 2020 Feb. 22 00:00

model was trained on a subdomain around an acoustic region of interest to ensure that the model captures the domain of influence with the relevant scales and dynamics. Furthermore, we demonstrated that the iLRDMD forecasts can be used for interdisciplinary applications such as underwater acoustics. It was shown that the error in transmission loss using the iLRDMD forecasts is acceptable and the sound channels were predicted at the correct locations. Finally, we demonstrated that the joint ocean-acoustics iLRDMD model can be used to provide onboard forecasts of ocean and acoustic fields with pre-specified acoustic characteristics.

Future work involves incorporating additional variables that influence the ocean dynamics in our adaptive reduced-order modeling. This includes atmospheric forcing that affect the ocean forecasting accuracy especially near the surface as well as open boundary conditions that vary in time and space. Other areas of ongoing work involves further sensitivity studies and new dynamic schemes for adapting various parameters within the iLRDMD algorithm. Establishing metrics for the errors that are most relevant for the application domain is also important for optimal reduced-order modeling. For example, being able to predict the presence of specific acoustic or ocean features can be more important than the exact position and time of these features. Other promising directions are interdisciplinary data assimilation [46], [47] directly within the iLRDMD framework as well as onboard Bayesian and machine learning [48]–[51].

ACKNOWLEDGMENTS

We thank our colleagues and friends at the Naval Research Laboratory - Stennis Space Center (J. Fabre, G. Jacobs, J. Metzger, and C. Trott), SRI International (D. Walker, P. Muscarella, and G. Marple), and our own MSEAS group for their collaboration and comments. We also thank the program managers Dr. William Schulz and Dr. Scott Harper for their inputs. We are grateful to the Office of Naval Research for partial support under the Tech Candidate grant N00014-21-1-2831 (Compression and Assimilation for Resource-Limited Operations) to the Massachusetts Institute of Technology (MIT).

REFERENCES

[1] P. F. J. Lermusiaux, P. J. Haley, Jr, and N. K. Yilmaz, "Environmental prediction, path planning and adaptive sampling: sensing and modeling for efficient ocean monitoring, management and pollution control," *Sea Technology*, vol. 48, no. 9, pp. 35–38, 2007.

[2] T. Ryu, M. Doshi, and P. F. J. Lermusiaux, "Time optimal path planning with adaptive reduced-order model ocean forecasts," *Journal of Marine Science and Engineering*, 2022, in preparation.

[3] T. Ryu, "Adaptive stochastic reduced-order modeling for autonomous ocean platforms," Master's thesis, Massachusetts Institute of Technology CAMBRIDGE, MASSACHUSETTES, inprep.

[4] J. P. Heuss, P. J. Haley, Jr., C. Mirabito, E. Coelho, M. C. Schönau, K. Heaney, and P. F. J. Lermusiaux, "Reduced order modeling for stochastic prediction onboard autonomous platforms at sea," in *OCEANS 2020 IEEE/MTS*. IEEE, Oct. 2020, pp. 1–10.

[5] J. P. Heuss, "Reduced order modeling for stochastic prediction and data assimilation onboard autonomous platforms at sea," Master's thesis, Massachusetts Institute of Technology and Woods Hole Oceanographic Institution, Cambridge, Massachusetts, Sep. 2021.

[6] J. N. Kutz, S. L. Brunton, B. W. Brunton, and J. L. Proctor, *Dynamic Mode Decomposition: Data-Driven Modeling of Complex Systems*. Philadelphia, Pennsylvania: SIAM, 2016.

[7] J. H. Tu, C. W. Rowley, D. M. Luchtenburg, S. L. Brunton, and J. N. Kutz, "On dynamic mode decomposition: Theory and applications," *Journal of Computational Dynamics*, vol. 1, no. 2, pp. 391–421, Jan. 2014.

[8] K. K. Chen, J. H. Tu, and C. W. Rowley, "Variants of dynamic mode decomposition: Boundary condition, koopman, and fourier analyses," *Journal of Nonlinear Science*, vol. 22, pp. 887–915, 2012.

[9] C. W. Rowley, S. B. Mezic, P. Schlatter, and D. S. Heningson, "Spectral analysis of nonlinear flows," *Journal of Fluid Mechanics*, vol. 641, pp. 115–127, Dec. 2009.

[10] P. J. Schmid, "Dynamic mode decompostion and of numerical and experimental data," *Journal of Fluid Mechanics*, vol. 656, pp. 5–28, Aug. 2010.

[11] T. Ryu, J. P. Heuss, P. J. Haley, Jr., C. Mirabito, E. Coelho, P. Hursky, M. C. Schönau, K. Heaney, and P. F. J. Lermusiaux, "Adaptive stochastic reduced order modeling for autonomous ocean platforms," in *OCEANS 2021 IEEE/MTS*. IEEE, Sep. 2021, pp. 1–9.

[12] R. Bleck, "An oceanic general circulation model framed in hybrid isopycnic-cartesian coordinates," *Ocean Modelling*, vol. 4, no. 1, pp. 55–88, 2002. [Online]. Available: https://www.sciencedirect.com/science/article/pii/S1463500301000129

[13] E. P. Chassignet, L. T. Smith, G. R. Halliwell, and R. Bleck, "North atlantic simulations with the hybrid coordinate ocean model (hycom): Impact of the vertical coordinate choice, reference pressure, and thermobaricity," *Journal of Physical Oceanography*, vol. 33, no. 12, pp. 2504 – 2526, 2003. [Online]. Available: https://journals.ametsoc.org/view/journals/phoc/33/12/1520-0485_2003_033_2504_naswth_2.0.co_2.xml

[14] N. Barton, E. J. Metzger, C. A. Reynolds, B. Ruston, C. Rowley, O. M. Smedstad, J. A. Ridout, A. Wallcraft, S. Frolov, P. Hogan *et al.*, "The navy's earth system prediction capability: A new global coupled atmosphere-ocean-sea ice prediction system designed for daily to subseasonal forecasting," *Earth and Space science*, vol. 8, no. 4, p. e2020EA001199, 2021.

[15] E. J. Metzger, R. W. Helber, P. J. Hogan, P. G. Posey, P. G. Thoppil, T. L. Townsend, A. J. Wallcraft, O. M. Smedstad, D. S. Franklin, L. Zamudo-Lopez, and M. W. Phelps, "Global ocean forecast system 3.1 validation test," 2017.

[16] J. Cummings, "Operational multivariate ocean data assimilation," *Quarterly Journal of The Royal Meteorological Society - QUART J ROY METEOROL SOC*, vol. 131, p. 23, 03 2006.

[17] J. Cummings and O. Smedstad, "Variational data assimilation for the global ocean," *Data Assimilation for Atmospheric, Oceanic and Hydrologic Applications*, vol. 2, pp. 303–343, 02 2013.

[18] S. Saha, S. Moorthi, H.-L. Pan, X. Wu, J. Wang, S. Nadiga, P. Tripp, R. Kistler, J. Woollen, D. Behringer, H. Liu, D. Stokes, R. Grumbine, G. Gayno, J. Wang, Y.-T. Hou, H.-Y. Chuang, H.-M. Juang, J. Sela, and M. Goldberg, "The ncep climate forecast system reanalysis," *Bulletin*

of The American Meteorological Society - BULL AMER METEOROL SOC, vol. 91, 08 2010.

[19] S. Saha, S. Moorthi, X. Wu, J. Wang, S. Nadiga, P. Tripp, D. Behringer, Y.-T. Hou, H.-Y. Chuang, M. Iredell, M. Ek, J. Meng, R. Yang, M. Peña, H. Dool, Q. Zhang, W. Wang, M. Chen, and E. Becker, "The ncep climate forecast system version 2," *Journal of Climate*, vol. 27, pp. 2185–2208, 03 2014.

[20] W. H. Ali, "Dynamically orthogonal equations for stochastic underwater sound propagation," Master's thesis, Massachusetts Institute of Technology, Computation for Design and Optimization Program, Cambridge, Massachusetts, Sep. 2019.

[21] W. H. Ali, M. S. Bhabra, P. F. J. Lermusiaux, A. March, J. R. Edwards, K. Rimpau, and P. Ryu, "Stochastic oceanographic-acoustic prediction and Bayesian inversion for wide area ocean floor mapping," in *OCEANS 2019 MTS/IEEE SEATTLE*. Seattle: IEEE, Oct. 2019, pp. 1–10.

[22] M. Alfatlawi and V. Srivastava, "An incremental approach to online dynamic mode decomposition for time-varying systems with applications to eeg data modeling," *Journal of Computational Dynamics*, vol. 7, no. 2, pp. 209–241, Jan. 2020.

[23] M. Brand, "Incremental singular value decomposition of uncertain data with missing values," in *Computer Vision — ECCV 2002*, A. Heyden, G. Sparr, M. Nielsen, and P. Johansen, Eds. Berlin, Heidelberg: Springer Berlin Heidelberg, 2002, pp. 707–720.

[24] G. M. Oxberry, T. Kostova-Vassilevska, W. Arrighi, and C. K., "Limited-memory adaptive snapshot selection for proper orthogonal decomposition," *International Journal for Numerical Methods in Engineering*, vol. 109, pp. 198–217, Jul. 2017.

[25] P. Lermusiaux, "Error subspace data assimilation methods for ocean field estimation: theory, validation and applications," Ph.D. dissertation, Harvard University, Cambridge, Massachusetts, Sep. 1997.

[26] P. F. J. Lermusiaux, "Estimation and study of mesoscale variability in the Strait of Sicily," *Dynamics of Atmospheres and Oceans*, vol. 29, no. 2, pp. 255–303, 1999.

[27] H. Zhang, C. W. Rowley, E. A. Deem, and L. N. Cattafesta, "Online dynamic mode decomposition for time-varying systems," 2017.

[28] P. F. J. Lermusiaux, "Evolving the subspace of the three-dimensional multiscale ocean variability: Massachusetts Bay," *Journal of Marine Systems*, vol. 29, no. 1, pp. 385–422, 2001.

[29] A. R. Robinson and P. F. J. Lermusiaux, "Prediction systems with data assimilation for coupled ocean science and ocean acoustics," in *Proceedings of the Sixth International Conference on Theoretical and Computational Acoustics*, A. Tolstoy et al, Ed. World Scientific Publishing, 2004, pp. 325–342, refereed invited Keynote Manuscript.

[30] J. Xu, P. F. J. Lermusiaux, P. J. Haley Jr., W. G. Leslie, and O. G. Logutov, "Spatial and Temporal Variations in Acoustic propagation during the PLUSNet-07 Exercise in Dabob Bay," in *Proceedings of Meetings on Acoustics (POMA)*, vol. 4. Acoustical Society of America 155th Meeting, 2008, p. 11.

[31] F.-P. A. Lam, P. J. Haley, Jr., J. Janmaat, P. F. J. Lermusiaux, W. G. Leslie, M. W. Schouten, L. A. te Raa, and M. Rixen, "At-sea real-time coupled four-dimensional oceanographic and acoustic forecasts during Battlespace Preparation 2007," *Journal of Marine Systems*, vol. 78, no. Supplement, pp. S306–S320, Nov. 2009.

[32] D. Wang, P. F. J. Lermusiaux, P. J. Haley, Jr., D. Eickstedt, W. G. Leslie, and H. Schmidt, "Acoustically focused adaptive sampling and on-board routing for marine rapid environmental assessment," *Journal of Marine Systems*, vol. 78, no. Supplement, pp. S393–S407, Nov. 2009.

[33] P. F. J. Lermusiaux, J. Xu, C.-F. Chen, S. Jan, L. Chiu, and Y.-J. Yang, "Coupled ocean–acoustic prediction of transmission loss in a continental shelfbreak region: Predictive skill, uncertainty quantification, and dynamical sensitivities," *IEEE Journal of Oceanic Engineering*, vol. 35, no. 4, pp. 895–916, Oct. 2010.

[34] T. F. Duda, W. G. Zhang, K. R. Helfrich, A. E. Newhall, Y.-T. Lin, J. F. Lynch, P. F. J. Lermusiaux, P. J. Haley, Jr., and J. Wilkin, "Issues and progress in the prediction of ocean submesoscale features and internal waves," in *OCEANS'14 MTS/IEEE*, 2014.

[35] T. F. Duda, Y.-T. Lin, A. E. Newhall, K. R. Helfrich, J. F. Lynch, W. G. Zhang, P. F. J. Lermusiaux, and J. Wilkin, "Multiscale multiphysics data-informed modeling for three-dimensional ocean acoustic simulation and prediction," *Journal of the Acoustical Society of America*, vol. 146, no. 3, pp. 1996–2015, Sep. 2019.

[36] P. F. J. Lermusiaux, P. J. Haley, Jr., C. Mirabito, W. H. Ali, M. Bhabra, P. Abbot, C.-S. Chiu, and C. Emerson, "Multi-resolution probabilistic ocean physics-acoustic modeling: Validation in the New Jersey continental shelf," in *OCEANS 2020 IEEE/MTS*. IEEE, Oct. 2020, pp. 1–9.

[37] P. F. J. Lermusiaux, C.-S. Chiu, and A. R. Robinson, "Modeling uncertainties in the prediction of the acoustic wavefield in a shelfbreak environment," in *Proceedings of the 5th International conference on theoretical and computational acoustics*, E.-C. Shang, Q. Li, and T. F. Gao, Eds. World Scientific Publishing Co., May 21-25 2002, pp. 191–200, refereed invited manuscript.

[38] P. F. J. Lermusiaux and C.-S. Chiu, "Four-dimensional data assimilation for coupled physical-acoustical fields," in *Acoustic Variability, 2002*, N. G. Pace and F. B. Jensen, Eds. Saclantcen: Kluwer Academic Press, 2002, pp. 417–424.

[39] P. F. J. Lermusiaux, "Uncertainty estimation and prediction for interdisciplinary ocean dynamics," *Journal of Computational Physics*, vol. 217, no. 1, pp. 176–199, 2006.

[40] C. Evangelinos, P. F. J. Lermusiaux, J. Xu, P. J. Haley, and C. N. Hill, "Many task computing for real-time uncertainty prediction and data assimilation in the ocean," *IEEE Transactions on Parallel and Distributed Systems*, vol. 22, no. 6, pp. 1012–1024, Jun. 2011, Special Section on Many-Task Computing.

[41] P. F. J. Lermusiaux, C. Mirabito, P. J. Haley, Jr., W. H. Ali, A. Gupta, S. Jana, E. Dorfman, A. Laferriere, A. Kofford, G. Shepard, M. Goldsmith, K. Heaney, E. Coelho, J. Boyle, J. Murray, L. Freitag, and A. Morozov, "Real-time probabilistic coupled ocean physics-acoustics forecasting and data assimilation for underwater GPS," in *OCEANS 2020 IEEE/MTS*. IEEE, Oct. 2020, pp. 1–9.

[42] A. Charous and P. F. J. Lermusiaux, "Dynamically orthogonal differential equations for stochastic and deterministic reduced-order modeling of ocean acoustic wave propagation," in *OCEANS 2021 IEEE/MTS*. IEEE, Sep. 2021, pp. 1–7.

[43] W. H. Ali and P. F. J. Lermusiaux, "Dynamically orthogonal equations for stochastic underwater sound propagation: Theory, schemes and applications," 2021, in preparation.

[44] ——, "Acoustics Bayesian inversion with Gaussian mixture models using the dynamically orthogonal field equations," 2021, in preparation.

[45] P. F. J. Lermusiaux, "Data assimilation via Error Subspace Statistical Estimation, part II: Mid-Atlantic Bight shelfbreak front simulations, and ESSE validation," *Monthly Weather Review*, vol. 127, no. 7, pp. 1408–1432, Jul. 1999.

[46] P. F. J. Lermusiaux, A. R. Robinson, P. J. Haley, and W. G. Leslie, "Advanced interdisciplinary data assimilation: Filtering and smoothing via error subspace statistical estimation," in *Proceedings of The OCEANS 2002 MTS/IEEE conference*. Holland Publications, 2002, pp. 795–802.

[47] P. F. J. Lermusiaux, "Adaptive modeling, adaptive data assimilation and adaptive sampling," *Physica D: Nonlinear Phenomena*, vol. 230, no. 1, pp. 172–196, 2007.

[48] P. Lu and P. F. J. Lermusiaux, "Bayesian learning of stochastic dynamical models," *Physica D: Nonlinear Phenomena*, vol. 427, p. 133003, Dec. 2021.

[49] A. Gupta and P. F. J. Lermusiaux, "Neural closure models for dynamical systems," *Proceedings of The Royal Society A*, vol. 477, no. 2252, pp. 1–29, Aug. 2021.

[50] P. J. Baddoo, B. Herrmann, B. J. McKeon, and S. L. Brunton, "Kernel learning for robust dynamic mode decomposition: linear and nonlinear disambiguation optimization," *Proceedings of the Royal Society A: Mathematical, Physical and Engineering Sciences*, vol. 478, no. 2260, p. 20210830, 2022. [Online]. Available: https://royalsocietypublishing.org/doi/abs/10.1098/rspa.2021.0830

[51] D. J. Alford-Lago, C. W. Curtis, A. T. Ihler, and O. Issan, "Deep learning enhanced dynamic mode decomposition," *Chaos: An Interdisciplinary Journal of Nonlinear Science*, vol. 32, no. 3, p. 033116, 2022.